  DOI 10.1515/HTMP.2011.054

Hydrolysis Rate of Aluminum Nitride in a Sodium Hydroxide Solution

Atsushi Nosaka,[1] **Takehito Hiraki,**[1]
Noriyuki Okinaka[2] **and Tomohiro Akiyama**[2,*]

[1] Graduate School of Engineering, Hokkaido University

[2] Center for Advanced Research of Energy and Materials, Faculty of Engineering, Hokkaido University, Sapporo, Japan

Abstract. This paper describes a kinetic analysis of the hydrolysis of aluminum nitride (AlN) powder under highly alkaline conditions, in which the temperature dependence of the hydrolysis rate was measured to derive the most suitable kinetic reaction model. The hydrolysis reaction, $AlN + NaOH + 3H_2O \rightarrow NaAl(OH)_4(aq) + NH_3$, $AlN + OH^- + 3H_2O \rightarrow Al(OH)_4^- + NH_3$, was experimentally monitored by the aluminum ion concentration measured via Inductively Coupled Plasma–Optical Emission Spectrometry (ICP-OES) at different constant temperatures of 295, 300, 305, 310, 316, and 327 K. The reaction accelerated exponentially with solution temperature. The time required for the complete dissolution of the AlN samples was highly dependent on temperature; it was 1 ks at 327 K and 120 ks at 295 K. Based on a comparative analysis of various kinetic models, the reaction curves were most successfully simulated by a second-order homogeneous reaction with an activation energy of 69.2 kJ mol^{-1}.

Keywords. Kinetics, aluminum nitride, hydrolysis, alkaline, sodium hydroxide, aluminum dross, second-order homogeneous reaction.

PACS®(2010). 65.40.-b.

1 Introduction

Aluminum nitride (AlN) is an important material in electronic packaging because of its excellent properties, including high thermal conductivity (320 W m^{-1} K^{-1}), high hardness, and low thermal expansion. In addition to commercially available AlN, *aluminum dross*, which is generated in the remelting process of waste aluminum, contains AlN as a major component. The hydrolysis of waste aluminum and aluminum dross using alkaline solution has been recently proposed [1–3] for the recycling of aluminum resources. Interestingly, we reported that pressurized hydrogen, together with a byproduct of aluminum hydroxide, could be generated successfully by the hydrolysis of waste *aluminum chips*. Although this was quite attractive from the viewpoint of a material-cycle society, the chemical compositions of aluminum chips and aluminum dross are essentially different; whereas the former does not contain AlN, the latter often contains as much as 25 mass% of AlN. This AlN generates ammonia by hydrolysis and causes smell pollution.

Over the last few years, several papers have been published on the mechanical and physical properties of AlN [4–7]. The kinetics between its powder and various solutions were also reported. For example, Reetz et al. [8] reported that at pH levels less than 7, the hydrolysis proceeds very slowly, even at elevated temperatures. Taylor and Lenie reported some properties of AlN, in which the corrosion rate of AlN powder in the acid solution is quite small, even at boiling temperature [9]. In addition, many papers have reported that the hydrolysis of AlN powder and substrates occurs in deionized water or moist air [8, 10–13]. Bowen et al. [13] found that the hydrolysis of AlN in water obeys first-order, surface chemical reaction kinetics, first producing a porous amorphous AlOOH that ultimately changes to crystalline $Al(OH)_3$. The hydrolysis rate of AlN powder in alkaline solution, as reported by Fukumoto et al. [14], was accelerated in a solution of NaOH compared to deionized water because of the catalytic property of NaOH. In this work, the hydrolysis was expressed by the following equation [15–21]:

$$AlN + NaOH + 3H_2O \rightarrow NaAl(OH)_4(aq) + NH_3, \quad (1)$$
$$(\Delta H^\circ, \Delta G^\circ) = (-175\ \text{kJ}, -206\ \text{kJ}).$$

In alkaline solutions, aluminum was dissolved in high pH solutions on the basis of the following potential pH equilibrium:

$$NaAl(OH)_4 + OH^- \rightarrow Al(OH)_4{}^- + NaOH, \quad (2)$$
$$(\Delta H^\circ, \Delta G^\circ) = (32\ \text{kJ}, 39\ \text{kJ}).$$

The aforementioned papers greatly contributed to elucidating the phenomena of AlN hydrolysis under different conditions. However, the kinetics of AlN powder hydrolysis are

Corresponding author: Tomohiro Akiyama, Center for Advanced Research of Energy and Materials, Faculty of Engineering, Hokkaido University, Kita 13 Nishi 8, Kita-ku, Sapporo 060-8628, Japan; E-mail: takiyama@eng.hokudai.ac.jp.

Received: January 7, 2011. Accepted: April 15, 2011.

not yet adequately explained, despite their significance in many engineering applications. Therefore, the purpose of this paper is to study the hydrolysis rate of pure AlN powder in a NaOH solution, by primarily examining the reaction mechanism, reaction rate constant, and activation energy. In experiments, the reaction rate was measured by monitoring the concentration of dissolved aluminum using inductively coupled plasma-optical emission spectrometry (ICP-OES), and the phase of the product was identified by an X-Ray Diffractometer (XRD) with Ni-filtered CuKα radiation.

2 Experimental Procedure

AlN powder (1.0 g; purity, 99.9 mass%; particle size, 1.2 μm; Kojyundokagaku, Japan) was introduced into 1000 mL of NaOH solution. To prepare the solution, grains of NaOH (purity, 99%; Kojyundokagaku, Japan) were dissolved in 1000 mL of deionized water with vigorous stirring. Table 1 lists the experimental conditions used in this study, where M_{AlN} is the number of moles of aluminum, and V_{NaOH}, C_{NaOH}, and T are the volume, concentration, and temperature of the NaOH solution, respectively.

During the experiments, care was taken to maintain the solution at a constant temperature of the desired values: 295, 300, 305, 310, 316, and 327 K. A water bath with an electric heater was used for this purpose. The amount of AlN (1.0 g) used, compared to the amount of solution (1000 mL), was sufficiently small to allow the influence of exothermic heat in Eq. (1) to be neglected. Each experiment was performed twice to measure the aluminum concentration of the solution periodically by ICP-OES, and to identify the hydrolyzed AlN using XRD and SEM. Samples for the measurement of ICP-OES were prepared according to the following procedure; a liquid sample of 5 mL was first taken from the solutions by a syringe, and then filtered using a syringe filter with a pore size of 0.2 μm to remove unreacted raw material. This procedure was repeated every 30 s until the end of the experiment. ICP-OES was available for the elemental analysis of NaOH solution without precipitate. The obtained data were used to evaluate the hydrolysis ratio from the following relationship:

$$\mathrm{AlN} + \mathrm{OH^-} + 3\mathrm{H_2O} \xrightarrow{\mathrm{NaOH}} \mathrm{Al(OH)_4^-} + \mathrm{NH_3}. \qquad (3)$$

The hydrolysis ratio, X_B, is expressed by

$$X_B = \frac{\text{Reacted AlN}}{\text{Initial AlN}} = \frac{W^0_{\mathrm{AlN}} - C_{\mathrm{Al^{3+}}} V_{\mathrm{NaOH}}}{W^0_{\mathrm{AlN}}}.$$

Here, $C_{\mathrm{Al^{3+}}}$ is the concentration of $\mathrm{Al^{3+}}$ (mol/mL); V_{NaOH}, the solution volume (mL); and W^0_{AlN}, the initial number of moles of AlN (mol).

Run	M_{AlN} (mol)	V_{NaOH} (ml)	C_{NaOH} (mol/l)	T (K)
a	0.024	1000	1.0	295
b	0.024	1000	1.0	305
c	0.024	1000	1.0	310
d	0.024	1000	1.0	316
e	0.024	1000	1.0	327
f	0.024	1000	0.5	300
g	0.024	1000	1.0	300
h	0.024	1000	1.5	300

Table 1. Experimental conditions for measuring the reaction rate between AlN and NaOH aqueous solution at different temperatures.

3 Results and Discussion

The measurements began immediately after the AlN powder was introduced into the NaOH solution in the reactor. Figure 1 shows the measured transient X_B values at 300 K for different NaOH concentrations. No appreciable reaction occurred in NaOH-free water. The reaction rate depended on the NaOH concentration. That is, it increased with the NaOH concentration up to 1.0 M NaOH; however, it did not depend solely on the concentration above this value. Reetz et al. [8] reported the same phenomenon in which mass transfer resistance for hydrolysis was negligible over 1.0 M NaOH. In fact, since the recycling process for waste

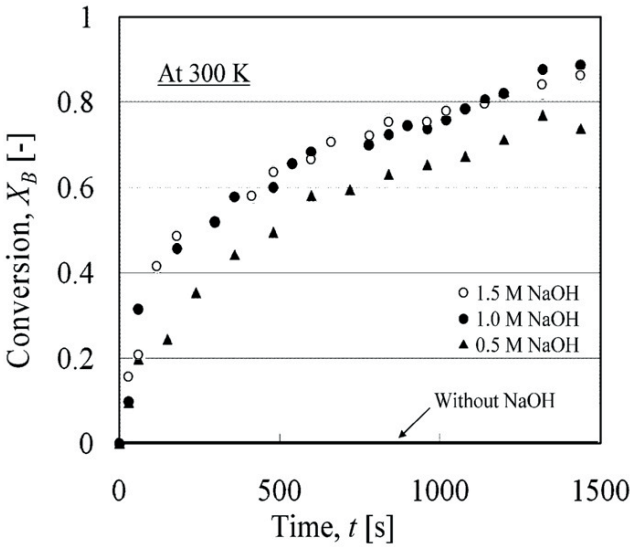

Figure 1. Effect of sodium hydroxide concentration on hydrolysis curves in which 1.0 g of aluminum nitride was introduced into 1000 mL of sodium hydroxide solution at 300 K.

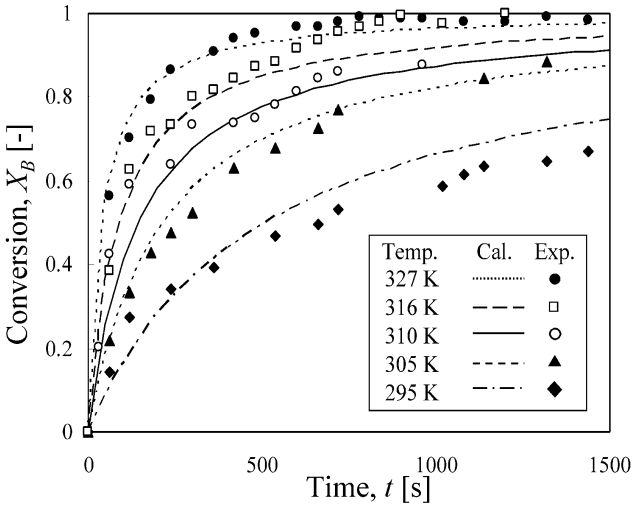

Figure 2. Observed and calculated conversion curves for 1.0 g of aluminum nitride dissolved in 1000 mL of sodium hydroxide solution at different constant temperatures of 295, 305, 310, 316, and 327 K.

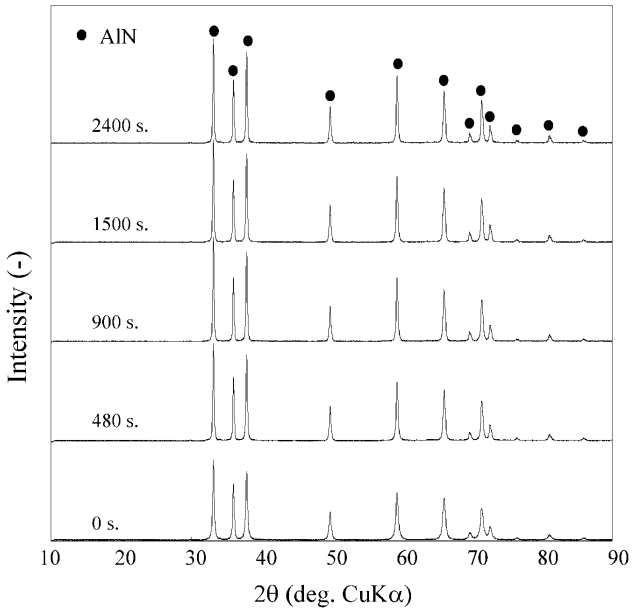

Figure 3. Changes in X-ray diffraction patterns of the material periodically recovered in the hydrolysis experiments, wherein 1.0 g of AlN powder was introduced into a sodium hydroxide solution of 1.0 M at 300 K, with sampling after 0, 480, 900, 1500, and 2400 s.

aluminum and aluminum dross was operated under high-pH conditions [1, 2], the NaOH concentration was fixed at 1.0 M in the runs of (a) to (e) listed in Table 1.

Figure 2 plots X_B versus the reaction time at different temperatures of 295, 305, 310, 316, and 327 K for the same 1.0 M NaOH solution. The results show strong temperature dependence of the reaction rate; for example, at 295 K, X_B was only 60% after 15 ks, whereas at 305 K, the reaction was complete in only 11 ks. During the experiments, the solution temperature was constant within ± 0.5 K.

Various equations have classically been proposed for solid–fluid reaction rate models (Table 2). Here, the models are expressed by the relationship between the reaction time t and X_B and grouped into three classes: unreacted core, shrinking sphere, and homogeneous reaction models. The observed data were plotted in an X-Y diagram according to the equation for each model, and the degree of fit was evaluated from the linearity of the plotted data using regression analysis. Table 2 also provides the determination coefficients for each model. Unreacted core models, apart from the ash diffusion model, and shrinking sphere models did not simulate the data well. Their determination factors were all less than 0.90.

Kinetic model.	Control step	Order	Expression	Determination coefficient, R^2(-)
Unreacted core	Film diffusion	—	$t/\tau = X_B$	0.519
	Ash diffusion	—	$t/\tau = 1\text{-}3(1\text{-}X_B)^{2/3}+2(1\text{-}X_B)$	0.971
	Reaction	1st	$t/\tau = 1\text{-}(1\text{-}X_B)^{1/3}$	0.816
Shrinking sphere	Film diffusion	—	$t/\tau = 1\text{-}(1\text{-}X_B)^{2/3}$	0.683
	Reaction	1st	$t/\tau = 1\text{-}(1\text{-}X_B)^{1/3}$	0.812
Homogeneous reaction	Reaction	1st	$kt = -\ln(1\text{-}X_B)$	0.889
	Reaction	2nd	$kt = X_B/[C_{AlNo}(1\text{-}X_B)]$	0.997

Table 2. Evaluated kinetic models expressed in terms of t-X_B, together with obtained determination coefficients used to simulate experimental data for the hydrolysis of AlN in 1.0 M NaOH at 305 K. Here, τ is a constant; k, the rate constant; X_B, the hydrolysis ratio; and t, the reaction time.

Two models showed good determination coefficients: the ash-diffusion-controlled unreacted core model ($R^2 = 0.971$) and the second-order homogeneous reaction model ($R^2 = 0.997$). However, the ash-diffusion-controlled unreacted core model is unreasonable because it does not agree at all with the phenomena observed in the experiments. In fact, *ash* did not generate around the particles.

Figure 3 shows the X-ray diffraction (XRD) patterns of samples recovered after 0, 480, 900, 1500, and 2400 s. Here, all of the detected peaks corresponded only to those of AlN. This indicates that no crystalline byproducts were generated around the AlN particles. In addition, D. Panias et al. [22] reported that the $Al(OH)_4^-$ complex ion is the predominant species at pH levels above 10. According to the measurements of the pH meter in the present experiments, the initial pH of 1 M NaOH(aq) was 13.35. Thus, we judged that only $Al(OH)_4^-$ exists as a stable phase under the present experimental conditions and that an amorphous phase did not generate around the particles. Therefore, the optimum model was determined from the maximum determination coefficient, R^2, as given in Table 2. The second-

order homogeneous reaction model ($R^2 = 0.997$) was selected as the optimum reaction model.

Figure 4 shows the kinetic analysis plots for second-order reactions from the experimental data for the hydrolysis of 1.0 g of aluminum nitride in a 1.0 M sodium hydroxide solution. The lines are plotted from a linear regression analysis of the experimental data. The second-order reaction is well known [23] and is represented by the following equation:

$$-r_{\mathrm{AlN}} = -\frac{dC_{\mathrm{AlN}}}{dt} = kC_{\mathrm{AlN}}^2, \tag{4}$$

where C_{AlN} is the concentration of AlN; C_{AlN}^* and C_{AlN}^0, the critical and initial concentrations of AlN, respectively; r_{AlN}, the hydrolysis rate of AlN; t, the reaction time; and k, the hydrolysis rate constant of AlN. Integrating Eq. (4) between concentrations C_{AlN}^0 and C_{AlN}^* and between times $\tau = 0$ and $\tau = t$ results in Eq. (5).

$$-\int_{C_{\mathrm{AlN}}^0}^{C_{\mathrm{AlN}}^*} \frac{dC_{\mathrm{AlN}}}{(C_{\mathrm{AlN}})^2} = k\int_0^t d\tau. \tag{5}$$

Equation (5) can be rewritten as follows:

$$1 - \frac{C_{\mathrm{AlN}}^*}{C_{\mathrm{AlN}}^0} = C_{\mathrm{AlN}}^* kt. \tag{6}$$

Here, X_B is given by the following equation:

$$X_B = 1 - \frac{C_{\mathrm{AlN}}^*}{C_{\mathrm{AlN}}^0}. \tag{7}$$

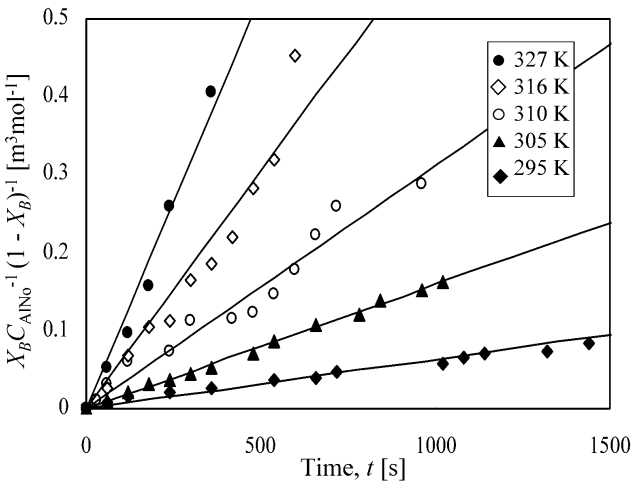

Figure 4. Kinetic analysis plots for second-order homogeneous reactions, with lines based on regression analysis, from the experimental data for the hydrolysis of 1.0 g of aluminum nitride in a 1.0 M sodium hydroxide solution.

Combining Eqs. (6) and (7), we have

$$\frac{1}{C_{\mathrm{AlN}}^0}\frac{X_B}{(1 - X_B)} = kt. \tag{8}$$

This shows a linear relationship between $1/C_{\mathrm{AlN}}^0$ and t. The straight lines in Figure 4 fit the data well. The k value was also calculated from the slope of the line.

The linearity of $\ln k$ versus T^{-1} is seen in the following equation:

$$\ln k = -\frac{E_a}{RT} + B. \tag{9}$$

Equation (9) can be written as

$$k = A\exp\left(-\frac{E_a}{RT}\right), \tag{10}$$

where E_a is the activation energy; R, the ideal gas constant (8.314 J mol^{-1} K^{-1}); B, a constant; and A, the pre-exponential factor.

Figure 5 shows the temperature dependence of the hydrolysis rate constant of AlN in 1.0 M NaOH calculated from the slope of the line in Figure 4. The data agreed well with Arrhenius' law and showed good linearity. The activation energy calculated from the slope of the line was $E_a = 69.2$ kJ mol^{-1}. In general, this value appears reasonable under the conditions of chemical reaction control. As a result, X_B is related to k and C_{AlN}^0 as shown in Eq. (11):

$$X_B = \frac{C_{\mathrm{AlN}}^0 tA\exp(-\frac{E_a}{RT})}{1 + C_{\mathrm{AlN}}^0 tA\exp(-\frac{E_a}{RT})}. \tag{11}$$

Introducing the values $C_{\mathrm{AlN}}^0 = 24.4$ mol m^3, $A = 1.2\times10^8$, $R = 8.314$ J mol^{-1} K^{-1}, and $E_a = 69.2$ kJ mol^{-1}, we can simulate the hydrolysis curve $X_B = F(t)$ at any desired

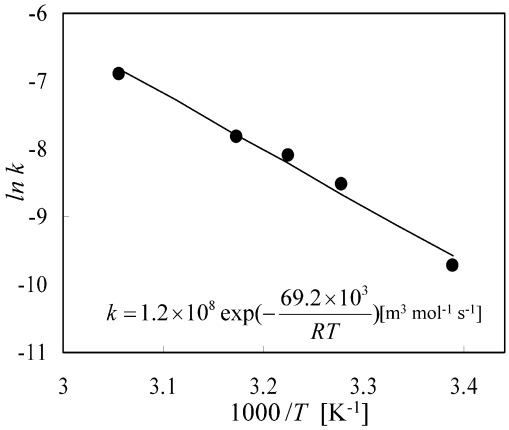

Figure 5. Temperature dependence of the rate constant for the hydrolysis of aluminum nitride in a 1.0 M sodium hydroxide solution.

temperature. Figure 2 also shows the hydrolysis curves calculated for 295, 305, 310, 316, and 327 K. These curves confirm that Eq. (11) simulates the measured data well.

4 Conclusions

The hydrolysis reaction of AlN in a NaOH solution at different temperatures was measured to derive the reaction rate equation. The reaction was expressed by $AlN + NaOH + 3H_2O \rightarrow NaAl(OH)_4(aq) + NH_3$ without the generation of a solid product. The following conclusions were obtained from the results and discussion.

(i) A NaOH solution concentration of 1.0 M was sufficient to remove mass transfer resistance in the boundary film around the particles when 1.0 g of AlN powder was introduced into 1000 mL of a NaOH solution ranging from 0.5 to 1.5 M in concentration.

(ii) Only $Al(OH)_4^-$ exists as a stable phase under the experimental conditions of this study. A comparative analysis of conventional reaction models revealed that the equation of the second-order homogeneous reaction model can simulate experimental data most successfully.

(iii) The rate constant of the hydrolysis reaction was well expressed by $k = 1.2 \times 10^8 \exp(-\frac{69.2\times10^3}{RT})$ [$m^3\ mol^{-1}\ s^{-1}$]. Here, the activation energy is 69.2 kJ mol^{-1}.

These results will be useful for understanding not only the AlN hydrolysis mechanism, but also the corrosion behavior of AlN in an alkaline solution. The kinetic data will be useful to analyze the treatment of aluminum dross involving generation of hydrogen and ammonia as a byproduct.

References

[1] T. Hiraki, M. Takeuchi, M. Hisa, T. Akiyama, Hydrogen production from waste aluminum at different temperatures, with LCA, *Materials Transactions*, **46** (2005), 1052–1057.

[2] T. Hiraki, S. Yamauchi, M. Iida, H. Uesugi, T. Akiyama, Process for recycling waste aluminum with generation of high-pressure hydrogen, *Environmental Science & Technology*, **41** (2007), 4454–4457.

[3] T. Hiraki, A, Nosaka, N, Okinaka, T, Akiyama, Synthesis of Zeolite-X from Waste Metals, *ISIJ Int.*, **49**(7) (2009), 1644–1648.

[4] M. E. Levinshtein, S. L. Rumyantsev, M. S. Shur (Eds.), *Chapter 2 in Properties of Advanced Semiconductors*, Wiley, New York, (2001).

[5] D. F. Lii, H. J. Lay, C. S. Ting, The mechanical properties of AlN/Al composite manufactured by squeeze casting, *J. Eur. Ceram. Soc.*, **22** (2002), 253–261.

[6] N. Nagendra, B. S. Rao, V. Jayaram, Microstructures and properties of Al_2O_3/Al-AlN composites by pressure less infiltration of Al-alloys, *Mater. Sci. Engg.*, **A 269** (1999), 26–37.

[7] R. Couturier, D. Ducret, P. Merle, J. P. Disson, P. Joubert, Elaboration and characterization of a metal matrix composite: Al/AlN, *J. Eur. Ceram. Soc.*, **17** (1997), 1861–1866.

[8] T. Reetz, B. Monch, M. Saupe, Aluminum nitride hydrolysis, *Ceramic Forum International*, **69** (1992), 464–465.

[9] K. M. Taylor, E. Lenie, Some properties of aluminum nitride, *J. Electrochem. Soc.*, **107** (1960), 308.

[10] Z. Liu, B. Huang. M. Gu, Corrosion behavior of Al/AlNp composite in alkaline solution, *Materials Letters*, **60** (2006), 2024–2028.

[11] R. Metselaar, R. Reenis, M. Chen, H. Gorter, H. T. Hintzen, Surface characterization of chemically treated aluminium nitride powders, *J. Eur. Ceram. Soc.*, **15** (1995), 1079–1085.

[12] A. Kocjan, K. Krnel, T. Kosmaè, The influence of temperature and time on the AlN powder hydrolysis reaction products, *J. Eur. Ceram. Soc.*, **28** (2008), 1003–1008.

[13] P. Bowen, J. G. Highfield, A. Mocellin, T. A. Ring, Degradation of aluminum nitride powder in aqueous environment, *J. Am. Ceram. Soc.*, **73**(1) (1990), 724–728.

[14] S. Fukumoto, T. Hookabe, H. Tsubakino, Hydrolysis behavior of aluminum nitride in various solutions, *J. Mater. Sci.*, **35** (2000), 2743–2748.

[15] I. Barin, O. Knacke, O. Kubaschewski, *Thermodynamical Properties of Inorganic Substances*, Springer-Verlag, Berlin and New York, NY, 1973, Supplement (1977).

[16] O. Knacke, O. Kubaschewski, K. Hesselman, *Thermochemical properties of inorganic substances, 2nd ed.*, Springer-Verlag, Berlin, (1991).

[17] M. W. Chase, C. A. Davies, J. R. Downey, Jr., D. J. Frurip, R. A. McDonald, and A. N. Syverud, *JANAF Thermochemical Tables Third Edition part II, Cr-Zr*, J. Phys. Chem. Ref. Data, **14**(1) (1985), 927–1856.

[18] B. Tagirov, J. Schott, Aluminum speciation in crustal fluids revisited, *Geochimica et Cosmochimica Acta*, **65**(21) (2001), 3965–3992.

[19] S. M. Bailey, K. L. Churney, R. L. Nuttall, The NBS tables of chemical thermodynamic properties, *J. of Phys. and Chem. Ref. Data*, **11**(2) (1982), 93–96.

[20] I. Diakonov, G. Pokrovski, P. Benezeth, J. Schott, J. Dandurand, J. Escalier, Gallium speciation in aqueous solution. Experimental study and modeling. Part I: Thermodynamic properties of $Ga(OH)_4$– to 300°C, *Geochim. Cosmochim. Acta*, **61**(4) (1997), 1333–1343.

[21] E. L. Shock, H. C. Helgeson, Calculation of the thermodynamic and transport properties of aqueous species at high pressures and temperatures: Correlation algorithms for ionic species and equation of state predictions to 5 kb and 1000°C, *Geochim. Cosmochim. Acta*, **52** (1988), 2009–2036.

[22] D. Panias, P. Asimidis, I. Paspaliaris, *Hydrometallurgy*, **59** (2001), 15–29.

[23] O. Leavenspiel, *Chemical Reaction Engineering 3rd edition*, Wiley, New York, 1998.